

FLOW ROUTING IN SYMMETRIC COMPOUND CHANNELS
BY APPARENT SHEAR FORCE MUSKINGUM-CUNGE METHOD
(대칭 복단면에서 ASF MUSKINGUM-CUNGE METHOD에 의한 하도추적)

전 무 갑*, Eli, R. N.**
Chun, Moo-Kab and Eli, R. N.

요 약: Muskingum-Cunge Method에 Apparent Shear Force(외부전단력)을 적용하여 대칭복합단면에 대한 하도추적 모델을 개발 하였다. 모델은 ASFMC라 불리며 모델내 하도추적이 수행되는 과정에서 중앙저수부와 홍수터 사이 발생하는 ASF가 고려 되었다. 모델의 또다른 특징은 비선형 매개변수가 적용 되었으며 모델의 결과는 DAMBRK와 기존의 방법인GPMC의 hydrographs와 비교되었다. ASFMC와 DAMBRK model 결과는 같은 경계조건및 입력값에 대해 거의같은 수문곡선을 발생시켰으나 GPMC의 결과는 상기2개의 model과는 상당한 차이를 보였다.

1. INTRODUCTION

The purpose of the research is to develop a new computer model called ASFMC(Apparent Shear Force Muskingum-Cunge Method) to predict open channel flow when the flow is routed in a symmetric compound channel.

The new computer model developed in the present work is based on the Muskingum-Cunge flow routing scheme[3,6]. The major new addition of the ASFMC model is the application of the Apparent Shear Force(ASF)[18] which results from momentum exchange in the turbulent flow between the deep main channel and the shallow floodplain.

In addition to the Apparent Shear Force, the model uses the nonlinear parameter method recommended by Ponce[6]. The test of the model is accomplished by comparing the flow-routing results at the downstream end of the prismatic channel with the equivalent hydrographs produced by DAMBRK(1988 version).

The above two results are also compared with the general routing practices of the Muskingum-Cunge Method(GPMC). The overall hydrograph shapes, peak discharges, and peak times of the new model are matched remarkably well with those of DAMBRK. However, considerable differences appeared between the results of the new model and GPMC.

2. BASIC EQUATIONS AND THEORIES

2.1 Muskingum-Cunge method

The kinematic wave equation is expressed as follows:

$$\frac{\partial Q}{\partial t} + (mv) \frac{\partial Q}{\partial x} = 0 \quad (1)$$

Cunge[3] discretized the Eq. (1) on the xt plane of Fig. 1 in a way that parallels the Muskingum method, centering the

* 정희원, 농어촌진흥공사 농어촌연구원 책임연구원

** Associate Prof., Dept. of Civil Engr. West Virginia Univ. Moagantown, WV. USA.

spatial derivative and off-centering the temporal derivative by means of a weighing factor X, and is expressed as follows [6]:

$$\frac{X(Q_j^{n+1} - Q_j^n) + (1-X)(Q_{j+1}^{n+1} - Q_{j+1}^n)}{\Delta t} + \frac{C(Q_{j+1}^n - Q_j^n) + (Q_{j+1}^{n+1} - Q_j^{n+1})}{2\Delta x} = 0 \quad (2)$$

The solution of above Eq. (2) for unknown flow rate Q at (n+1), (j+1) gives as follows:

$$Q_{j+1}^{n+1} = C_1 Q_j^n + C_2 Q_j^{n+1} + C_3 Q_{j+1}^n \quad (3)$$

By application cell Reynolds number[6] and Courant number [1,6], the routing coefficients C1, C2, and C3 lead to the following[6]:

$$C_1 = \frac{1 + C - D}{1 + C + D}, \quad C_2 = \frac{-1 + C + D}{1 + C + D}, \quad C_3 = \frac{1 - C + D}{1 + C + D} \quad (4)$$

As explained in Eq. (3), the unknown flow rate is computed by the routing coefficients on the known values, and these coefficients are absolutely decided by the values of the cell Reynolds number D and the Courant number C as shown in Eq. (13).

On the other hand, the cell Reynolds and the Courant number depends on the flow properties such as discharge and velocity.

The flow properties of the simple cross-section can be computed by simple application of the various kinds of well known methods such as Manning equation, Chezy equation, Darcy-Weisbach formula, etc.,. In compound channels, however, there are too many flow complexities to apply these equations properly as will be explained in the next section.

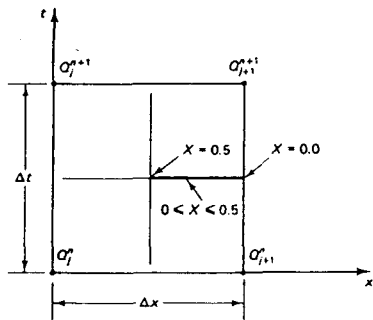


Figure 1 Space-Time Descretization of Kinematic Wave Equation Paralleling Muskingum-Cunge Method[6]

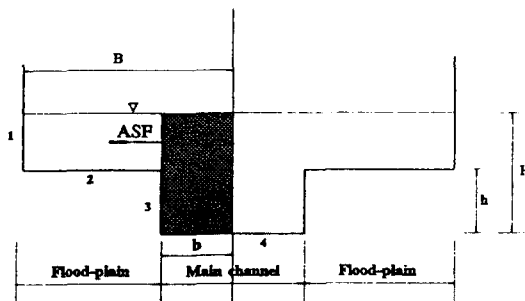


Figure 2 Typical Symmetric Compound Cross-Section

2.2 Flow Properties of Compound Cross-Sections

The actual average velocity equations for each sub-cross section of symmetric compound cross-section as shown in Fig. 2

are as follows:

$$v_m = \frac{1.49}{n_m \sqrt{g}} R_m^{1/6} \sqrt{\frac{\tau_m}{\rho}} \quad v_f = \frac{1.49}{n_f \sqrt{g}} R_f^{1/6} \sqrt{\frac{\tau_f}{\rho}} \quad (5)$$

The value of shear stress must be obtained from the actual shear force of main channel and floodplain sub-cross section. In order to calculate the actual shear force on the floodplain, the apparent shear force is added to undisturbed shear force. On the other hand, the main channel shear force is decreased as much as the apparent shear forces on both intersections in the symmetric compound section.

Therefore, the actual average shear stress in the main channel and floodplain sub-cross section of a symmetric cross-section shown in Fig. 2 is expressed as bellows:

$$\tau_m = \frac{SF_m - 2S_A}{2p_3 + p_4} \quad \tau_f = \frac{SF_f - S_A}{p_1 + p_2} \quad (6)$$

2.3 Apparent shear force(ASF)

Knight et al[4] studied the influence of differential roughness between the floodplain and main channel on the momentum transfer process, and presented a practical equation concerning the apparent shear force on the basis of roughness and geometry condition of a symmetrical compound cross-section.

In a symmetric cross-section as shown in Fig. 2, the percentage of apparent shear force may be expressed as follows[5]:

$$\%S_A = \frac{50}{(\alpha-1)\beta + 1} - \frac{1}{2} [100 - \%2(SF_1 + SF_2)] \quad (7)$$

Therefore, the absolute value of apparent shear force s_a in lb/ft may be obtained simply by multiplying the total shear force of whole cross-section, SFT, by $\%s_a$ as follows:

$$s_a = SFT \times (\%s_a/100) \quad (8)$$

On the other hand, Knight's experimental equation[5] developed by physical hydraulic tests is applied to compute the shear force percentage on the both floodplains, $\%2[SF_1 + SF_2]$ of Eq. (7). It is as follows:

$$\%2(SF_1 + SF_2) = 48.0(\alpha - 0.8)^{0.289} (2\beta)^{1/\omega} (1 + 1.02\beta^{1/2}\log_{10}\gamma) \quad (9)$$

As shown in Eq.(9), the percentage of the total shear force carried by floodplains, $\%2[SF_1 + SF_2]$, is increased with the floodplain width, water depth, and floodplain roughness.

2.4 Variable Computational Increment

A variable computational time increment scheme is applied. Initially, a large time increment DT is selected. Then the time increment DT is further refined according to the rate of

upstream inflow change.

As shown in Fig. 3, the time increment in each computational cell may be different. If an abrupt flow change rate is sensed, the current time increment is reduced; if a gradual change is found, the size of time increment is increased. For the selection of the spatial increment, the model follows the Ponce's accuracy criteria on Δx [6] expressed as follows:

$$\Delta x \leq \frac{1}{\lambda} (\Delta x_c + \Delta x_D) \quad (10)$$

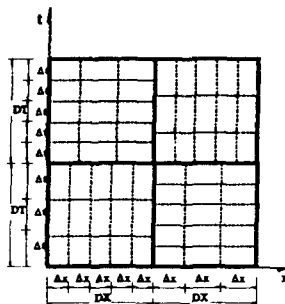


Figure 3 Definition Sketch of Variable Time and Spatial Increment

3. RESULTS AND DISCUSSIONS

For the testing and validation of the ASFCM, several cross-sections have been hypothesized as shown in Fig. 4. The

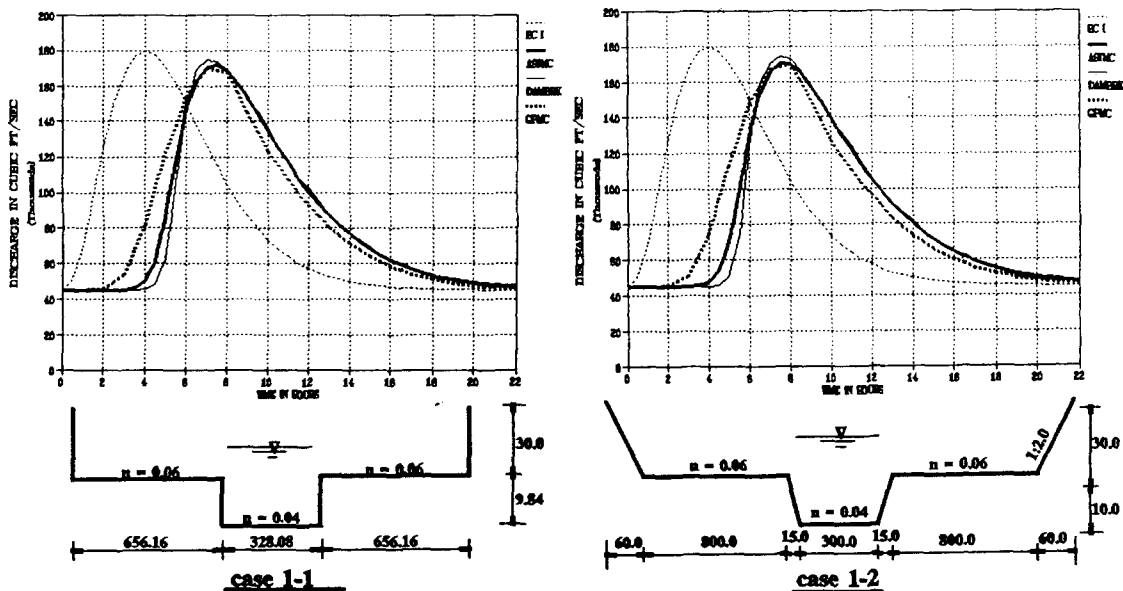


Figure 4 Schematic of Test Cross-Sections and Hydrographs

results of ASFMC routings are matched remarkably well with those of the equivalent routings of DAMBRK as shown in Fig. 4. The consistency of the peak time and peak discharge has been demonstrated in the comparative testing. The routing results of GPMC, however, are shown to be considerably different from those of the above two models.

The maximum RMS(%) errors between the ASFMC and DAMBRK on the routed hydrograph are 5.07%, 5.46%, and 2.85%, respectively. However, as shown in the plotted hydrographs of Fig. 4, all errors between the ASFMC and DAMBRK are mainly from the disparities at the rising limb where the abrupt flow changes are occurring as explained above. The plots of routed hydrographs of the GPMC are also shown in the same figure.

4. CONCLUSIONS

From the present investigations, the following conclusions have resulted;

- The hydrographs produced by the ASFMC are matched closely to those of the DAMBRK.
- Comparing the hydrographs produced by the ASFMC and DAMBRK models, the consistency of the hydrograph characteristics, such as peak discharge and peak time, are also demonstrated with reasonable hydraulic responses according to the geometric conditions.
- The routed hydrographs of the GPMC show earlier rising and falling limbs and have significantly greater differences as compared to those from ASFMC. This is a reasonable hydraulic phenomenon, because the flows of the ASFMC are resisted more than the flows of the GPMC due to the kinematic effect.

NOMENCLATURE

Symbol	Definition
A	area of whole cross-section
C	Courant number
C ₁	routing coefficient of Eq. (4)
C ₂	routing coefficient of Eq. (4)
C ₃	routing coefficient of Eq. (4)
c	wave speed
D	cell Reynolds number
g	gravity acceleration
m	exponent coefficient
n _f	Manning's roughness coefficient for a floodplain
n _m	Manning's roughness coefficient for a main channel
p ₁	wetted perimeter of a floodplain wall
p ₂	wetted perimeter of a floodplain bed
p ₃	wetted perimeter of a main channel wall
p ₄	wetted perimeter of a main channel bed
Q	discharge
R _f	hydraulic radius of a floodplain
R _m	hydraulic radius of a main channel
S _m	sinuosity factor
S _r	energy slope

s_o	gravity slope
SF_f	shear force in a floodplain
SF_m	shear force in a main channel
SF_1	actual shear force in a floodplain bed
SF_2	actual shear force in a floodplain wall
S_A	apparent shear force on the vertical interface
$\%S_A$	percentage of apparent shear force on the vertical interface
$\%[SF_1+SF_2]$	the percentage of acting shear force in a floodplain
t	time
Δt	time interval
v	velocity
v_f	actual average velocity of a floodplain
v_m	actual average velocity of a main channel
X	routing parameter(dimensionless weighing factor)
x	distance in flow direction
Δx	spatial interval
Δx_c	minimum subreach length
Δx_D	maximum subreach length
α	non-dimensional width parameter, (B/b)
β	non-dimensional depth parameter, $(H-h)/H$
γ	n_f/n_m
λ	accuracy parameter
ρ	density
τ_f	actual average shear stress in a floodplain
τ_m	actual average shear stress in a main channel
ω	$0.75 e^{0.38\alpha}$

REFERENCES

1. Abbot, M. B. and Basco, D. R. Computational Fluid Dynamics, 1990, Longman Scientific & Technical and John Wiley & Sons, Inc., New York, NY.
2. Chow, V. T., Maidment, D. R., and Mays, L. W., Applied Hydrology, 1988, McGraw-Hill, New York, NY.
3. Cunge, "On the Subject of a Flood Propagation Computation Method(Muskingum Method)." Journal of Hydraulic Research, International Association for Hydraulic Research(IAHR), Vol.7, No. 2, 1969, pp. 205-230.
4. Knight, D. W., Demetriou, J. D., and Hamed, M. E. " Flood Plain and Main Channel Flow Interaction." Journal of Hydraulic Engineering, ASCE, Vol. 109, No. 8, August, 1983, pp. 1073-1091.
5. Knight, D. W. and Hamed, M. E. " Boundary Shear in Symmetrical Compound Channels." Journal of Hydraulic Engineering, ASCE, Vol. 110, No. 10, Oct, 1984, pp. 1412-1429.
6. Ponce, V. M., Engineering Hydrology, 1989, Prentice Hall, Englewood Cliffs, NJ.